frontiers in Plant Science

ORIGINAL RESEARCH
published: 24 November 2016
doi: 10.3389/fpls.2016.01769

The Sclerophyllous *Eucalyptus camaldulensis* and Herbaceous *Nicotiana tabacum* Have Different Mechanisms to Maintain High Rates of Photosynthesis

Wei Huang[1,2]*, *You-Gui Tong*[3], *Guo-Yun Yu*[3] *and Wei-Xian Yang*[3]

[1] *Key Laboratory of Tropical Forest Ecology, Xishuangbanna Tropical Botanical Garden, Chinese Academy of Sciences, Mengla, China,* [2] *Department of Economic Plants and Biotechnology, Kunming Institute of Botany, Chinese Academy of Sciences, Kunming, China,* [3] *Forestry Bureau of Dongchuan County, Kunming, China*

It is believed that high levels of mesophyll conductance (g_m) largely contribute to the high rates of photosynthesis in herbaceous C_3 plants. However, some sclerophyllous C_3 plants that display low levels of g_m have high rates of photosynthesis, and the underlying mechanisms responsible for high photosynthetic rates in sclerophyllous C_3 plants are unclear. In the present study, we examined photosynthetic characteristics in two high-photosynthesis plants (the sclerophyllous *Eucalyptus camaldulensis* and the herbaceous *Nicotiana tabacum*) using measurements of gas exchange and chlorophyll fluorescence. Under saturating light intensities, both species had similar rates of CO_2 assimilation at 400 μmol mol^{-1} CO_2 (A_{400}). However, *E. camaldulensis* exhibited significantly lower g_m and chloroplast CO_2 concentration (C_c) than *N. tabacum*. A quantitative analysis revealed that, in *E. camaldulensis*, the g_m limitation was the most constraining factor for photosynthesis. By comparison, in *N. tabacum*, the biochemical limitation was the strongest, followed by g_m and g_s limitations. In conjunction with a lower C_c, *E. camaldulensis* up-regulated the capacities of photorespiratory pathway and alternative electron flow. Furthermore, the rate of alternative electron flow was positively correlated with the rates of photorespiration and ATP supply from other flexible mechanisms, suggesting the important roles of photorespiratory pathway, and alternative electron flow in sustaining high rate of photosynthesis in *E. camaldulensis*. These results highlight the different mechanisms used to maintain high rates of photosynthesis in the sclerophyllous *E. camaldulensis* and the herbaceous *N. tabacum*.

Keywords: alternative electron flow, CO_2 assimilation, mesophyll conductance, photorespiration, sclerophyllous

OPEN ACCESS

Edited by:
Antonio Ferrante, University of Milan, Italy

Reviewed by:
Veronica De Micco, University of Naples Federico II, Italy
Daniele Massa, Council for Agricultural Research and Economics, Italy

***Correspondence:**
Wei Huang
huangwei@mail.kib.ac.cn

Specialty section:
This article was submitted to Plant Physiology, a section of the journal Frontiers in Plant Science

Received: *04 August 2016*
Accepted: *10 November 2016*
Published: *24 November 2016*

Citation:
Huang W, Tong Y-G, Yu G-Y and Yang W-X (2016) The Sclerophyllous Eucalyptus camaldulensis and Herbaceous Nicotiana tabacum Have Different Mechanisms to Maintain High Rates of Photosynthesis. Front. Plant Sci. 7:1769. doi: 10.3389/fpls.2016.01769

INTRODUCTION

In C_3 plants, rates of photosynthesis differ widely among species. For individual leaves or whole plants, photosynthetic capacity mainly depends upon their biochemical composition and morphology. Generally, plants with high rates of CO_2 assimilation have higher levels of cytochrome *f*, ATP synthase, Rubisco, and other Calvin-Benson cycle enzymes (Evans, 1987; Terashima and Evans, 1988; Hikosaka, 1996; Hikosaka and Terashima, 1996; Yamori et al., 2010, 2011). The rate of

CO_2 assimilation is maximized in leaves that usually have high levels of stomatal conductance (g_s) and mesophyll conductance (g_m), which increase CO_2 diffusion into the chloroplasts (Yamori et al., 2010, 2011). Herbaceous plants, e.g., tobacco (*Nicotiana tabacum*), spinach (*Spinacia oleracea*), rice (*Oryza sativa*), and *Triticum aestivum* have commonly been used for studying the mechanism of photosynthetic acclimation and the rate-limiting step for CO_2 assimilation. In herbaceous C_3 plants, the rate-limiting step of photosynthesis depends on leaf N content and is mainly determined by N portioning between Rubisco and photosynthetic electron transport (Yamori et al., 2011). However, little is known about the coordination of photosynthetic electron flow and gas exchange in sclerophyllous plants that have high rates of photosynthesis. What is more, it is still not well understood whether the mechanisms responsible for high rates of photosynthesis vary among sclerophyllous and herbaceous C_3 plants.

Leaf anatomy plays an important role in determining photosynthetic capacity. The area of chloroplasts facing the intercellular space largely determines the light-saturated rate of photosynthesis (Oguchi et al., 2003, 2005). High-photosynthesis herbaceous plants usually have thinner cell walls, leading to high values of g_m. By comparison, leaves of sclerophyllous plants have thicker cell walls, with a high leaf dry mass per area (LMA) (Hassiotou et al., 2009). As an important morphological trait, LMA is inversely related to g_m in sclerophyllous plants (Hassiotou et al., 2009). Therefore, sclerophyllous plants usually have low g_m and slow rates of photosynthesis (Loreto et al., 1992). For example, a sclerophyllous species *Quercus guyavifolia* has a low rate of the maximum photosynthesis being 13 μmol CO_2 m^{-2} s^{-1} (Huang et al., 2016). As we known, the sclerophyllous species *Eucalyptus camaldulensis* has been introduced for production of paper in China due to its high rate of photosynthesis. The high value of LMA for leaves of *E. camaldulensis* is assumed to result in low g_m. Mesophyll conductance plays an important role in determining the rate of photosynthesis in C_3 plants (Flexas et al., 2008; Carriqui et al., 2015). A low g_m value increases the resistance of CO_2 conductance to the chloroplasts, leading to a decline in the chloroplast CO_2 concentration (C_c) and, thus, restricted CO_2 assimilation (Loreto et al., 1992; Hanba et al., 2002; Flexas et al., 2012; Gago et al., 2013; Carriqui et al., 2015). Therefore, for the sclerophyllous *E. camaldulensis*, other mechanisms favoring CO_2 diffusion must be used to increase C_c because it is essential for the maintenance of high CO_2 assimilation.

The net rate of CO_2 assimilation (A_n) is largely dependent upon the value of C_c because the latter directly determines the affinity of Rubisco to CO_2 or O_2 (Farquhar et al., 1980; von Caemmerer, 2000). An increased C_c increases the rate of RuBP carboxylation and, thus, results in a rise in the photosynthetic rate. As shown by the calculation of $C_c = C_i - A_n/g_m$, C_c is mainly determined by three factors: intercellular CO_2 concentration (C_i), A_n, and g_m. During the steady-state phase under high light, A_n and g_m reach the steady-state values, the value of C_i determines C_c principally but is mainly influenced by g_s. Stomata are the channels for gas exchange between leaf and atmosphere. During periods of drought or high temperatures, a decrease in g_s leads to an inhibition of the Calvin-Benson cycle (Flexas et al., 2002; Flexas and Medrano, 2002). In herbaceous plants of high values of g_m, high rates of photosynthesis are usually accompanied by high values of g_s (Yamori et al., 2010, 2011). However, it is unclear whether the high-photosynthesis sclerophyllous plant *E. camaldulensis* elevate g_s to remedy the deficiency of g_m.

According to the C_3 photosynthesis model, photosynthesis can be limited by RuBP carboxylation and/or RuBP regeneration (Farquhar et al., 1980). When C_c is higher than C_{trans} (the chloroplast CO_2 concentration at which the transition from RuBP carboxylation limitation to RuBP regeneration limitation occurs), then CO_2 assimilation is limited by RuBP regeneration (Yamori et al., 2010, 2011). Once C_c is lower than C_{trans}, CO_2 assimilation tends to be limited by RuBP carboxylation. In herbaceous *N. tabacum* plants grown at high nitrogen concentration, the rate-limiting step of CO_2 assimilation is RuBP regeneration because C_c is greater than C_{trans} (Yamori et al., 2010, 2011). In the sclerophyllous *E. camaldulensis*, the high rate of photosynthesis and low g_m can cause C_c to be less than C_{trans}. Consequently, the rate of CO_2 assimilation is probably limited by RuBP carboxylation in *E. camaldulensis*. If this occurs, then the reduced C_c drives increased photorespiration (or RuBP oxygenation). The photorespiratory pathway is essential for photosynthesis at normal atmospheric CO_2 concentrations (Chastain and Ogren, 1989; Eisenhut et al., 2007), and impairment of that pathway decreases the rate of photosynthesis under such CO_2 conditions (Somerville and Ogren, 1980, 1981, 1983; Takahashi et al., 2007).

Enhancement of the photorespiratory pathway leads to a considerably improved net photosynthetic rate in *Arabidopsis thaliana* (Timm et al., 2012, 2015). Therefore, we might also speculate that *E. camaldulensis* enhances the capacity of that pathway to favor the Calvin-Benson cycle. Furthermore, if the photorespiratory pathway is up-regulated in plants of *E. camaldulensis*, then the stoichiometry of the ATP/NADPH energy demand by primary metabolism will increase. Therefore, such plants must utilize other flexible mechanisms to balance the ATP/NADPH ratio, e.g., cyclic electron flow (CEF) around photosystem I (PSI) or the water-water cycle (Makino et al., 2002; Walker et al., 2014). The WWC channels electrons obtained from splitting of water molecules at PSII. These electrons are transported to oxygen via the Cyt b_6/f complex and PSI, resulting in the formation of a proton gradient across the thylakoid membranes (Asada, 1999, 2000). However, little is known about how the WWC functions in the high-photosynthesis sclerophyllous plant *E. camaldulensis*.

N. tabacum is regarded as a model plant to study the mechanisms of photosynthetic regulation for herbaceous plants. However, it is not known how the sclerophyllous plant *E. camaldulensis* obtain a high rate of photosynthesis. Here, we compared g_s, g_m, CO_2 assimilation, photorespiration, and alternative electron flow between *N. tabacum* and *E. camaldulensis*. Our objective was to examine the potential differences in mechanisms underlying high rates of photosynthesis between herbaceous and sclerophyllous plants.

MATERIALS AND METHODS

Plant Materials and Growth Conditions

We compared the photosynthetic characteristics of *N. tabacum* and *Eucalyptus camaldulensis* Dehnh. The latter is a fast-growing species native to Australia that has been widely introduced into China for forest plantations. For this study, *Eucalyptus* samples were collected from plants grown in an open field at an elevation of 700 m in Dongchuan County, Kunming City, Yunnan Province, China. The monthly air temperature, total radiation and precipitation were displayed in **Figure 1** (data were collected from 1961 to 1980). Seedlings of *N. tabacum* cv. k326 were cultivated in plastic pots in a phytotron at Kunming Institute of Botany, Yunnan, China. Growing conditions were 24/18°C (day/night), 60% relative humidity, and an atmospheric CO_2 concentration maintained at 400 μmol mol^{-1}. The phytotron used sunlight as the source of illumination, and plants were exposed to approximately 95% of full sunlight (maximum at noon ≈ 1990 μmol photons m^{-2} s^{-1}). Photosynthetic parameters were measured in June of 2014. Measurements were made using four mature leaves from four independent plants per species. Fully expanded mature leaves on 13-week-old plants of *N. tabacum* were used for photosynthetic measurements. For *E. camaldulensis*, mature leaves that flushed in the spring on 3-year-old plants were used for measurements.

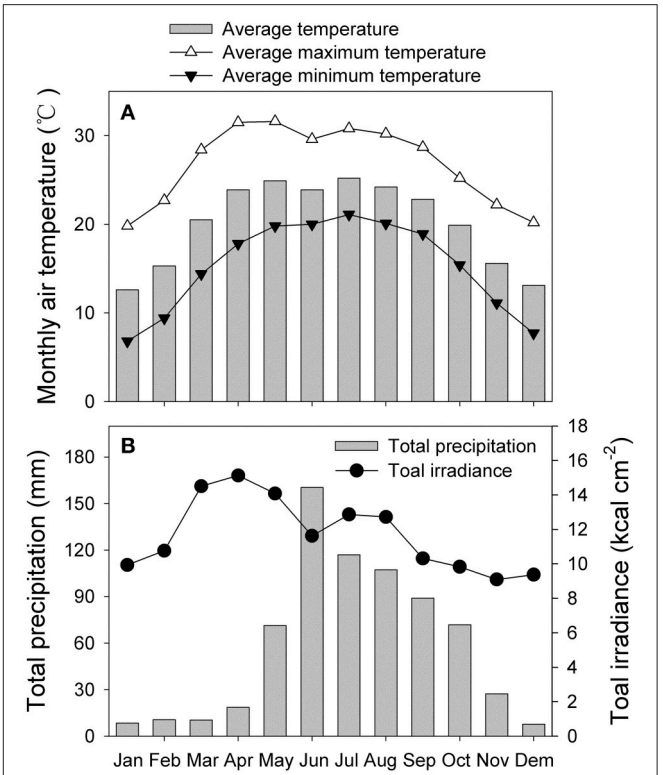

FIGURE 1 | Monthly climatic data collected from 1961 to 1980. (A) monthly average air temperature, monthly average maximum and minimum temperatures; **(B)** monthly precipitation and total irradiance.

Measurements of Gas Exchange and Chlorophyll Fluorescence

Photosynthetic parameters for gas exchange and chlorophyll fluorescence were monitored with an open gas exchange system that incorporated infrared CO_2 and water vapor analyzers (Li-6400XT; Li-Cor Biosciences, Lincoln, NE, USA) and a 2-cm^2 measuring head (6400-40 Leaf Chamber Fluorometer; Li-Cor Biosciences). Data were recorded at 25°C and a relative air humidity of 60–70%. The atmospheric CO_2 concentration was maintained at 400 μmol mol^{-1} by the Li-6400XT. Both g_s and the CO_2 assimilation rate peaked after plants were exposed to saturating light (2000 μmol photons m^{-2} s^{-1}) for 20 min. Immediately, light response curves were evaluated at 2-min intervals at different light intensities. For *N. tabacum*, light response curves were measured at a photosynthetic photon flux density (PPFD) of 2000, 1600, 1200, 1000, 800, 600, 400, 300, 200, 150, 100, 50, or 0 μmol photons m^{-2} s^{-1}. For *E. camaldulensis*, light response curves were measured at a photosynthetic photon flux density (PPFD) of 2000, 1600, 1200, 1000, 800, 500, 300, 150, 100, 50, or 0 μmol photons m^{-2} s^{-1}.

The fluorescence parameters F_m' and F_s were evaluated as previously described (Baker and Rosenqvist, 2004), with F_m' representing the maximum fluorescence after light-adaption and F_s being the light-adapted steady-state fluorescence. The effective quantum yield of PSII was calculated as $\Phi_{PSII} = (F_m' - F_s)/F_m'$ (Genty et al., 1989). The maximum fluorescence after dark adaptation (F_m) was examined after 30 min of dark adaptation following measurement of the light response curve. Non-photochemical quenching was calculated as NPQ = $(F_m - F_m')/F_m'$.

Estimation of Photosynthetic Electron Flow

Using the data of chlorophyll fluorescence parameters, total photosynthetic electron flow through PSII is calculated as follows (Krall and Edwards, 1992):

$$J_T = \Phi_{PSII} \times PPFD \times L_{abs} \times 0.5$$

where Φ_{PSII} is the effective quantum yield of PSII and L_{abs} represents leaf absorbance. We applied the constant of 0.5 based on the assumption that photons were equally distributed between PSI and PSII.

Using the basic equation of leaf carbon dioxide gas exchange and Rubisco specificity for carboxylation relative to oxygenation (von Caemmerer and Farquhar, 1981; Sharkey, 1988; Walker et al., 2016), the rate of Rubisco carboxylation (V_c) and that of Rubisco oxygenation (V_o) are calculated according to.

$$V_c = \frac{A_n + R_d}{1 - (\Gamma^*/C_c)}$$

$$V_o = \frac{A_n + R_d}{(C_c/2\Gamma^*) - 0.5}$$

where A_n represented the net rate of CO_2 assimilation, R_d was the rate of mitochondrial respiration as measured after 30 min of dark adaptation, Γ^* was the CO_2 compensation point in the absence of daytime respiration (Farquhar et al., 1980; Brooks and

Farquhar, 1985), and C_c was the chloroplast CO_2 concentration. The electron flow for photorespiratory carbon oxidation can be expressed as:

$$Je\,(\mathrm{PCO}) = 4 \times V_o$$

The NADPH demands from CO_2 assimilation and photorespiration were calculated according to the models of Farquhar et al. (1980). Using the data from gas exchange measurements, we determined the rate of electron transport for NADPH required by carboxylation and oxygenation of RuBP (J_g) as follows (Zivcak et al., 2013; Walker et al., 2014)

$$J_g = 4 \times (A_n + R_d) \times \left(C_i + 2\Gamma^*\right)/(C_i - \Gamma^*)$$

where C_i was the intercellular CO_2 concentration. The alternative electron flow was calculated as follows (Makino et al., 2002; Zivcak et al., 2013; Huang et al., 2016):

$$J_a = J_T - J_g$$

Estimations of Mesophyll Conductance and Chloroplast CO_2 Concentration

Values for mesophyll conductance (g_m) were estimated through a combination analysis of gas exchange and chlorophyll fluorescence, and according to the following equation (Harley et al., 1992; Loreto et al., 1992; Warren and Dreyer, 2006; Yamori et al., 2010, 2011):

$$g_m = \frac{A_n}{C_i - \Gamma^*(J_T + 8\,(A_n + R_d))/(J_T - 4\,(A_n + R_d))}$$

Using the estimated g_m, we calculated the chloroplast CO_2 concentration (C_c) according to the following equation (Long and Bernacchi, 2003; Warren and Dreyer, 2006; Yamori et al., 2010, 2011):

$$C_c = C_i - \frac{A_n}{g_m}$$

The response of net CO_2 assimilation rate to CO_2 concentration was examined at 2000 μmol photons m^{-2} s^{-1} and 25°C. Before A/C_i measurement, leaves were light adapted at 2000 μmol photons m^{-2} s^{-1} and 400 μmol mol^{-1} CO_2 concentration for at least 20 min to obtain the maximum values of g_s and A_n. Afterwards, the CO_2 concentrations were set to 50 μmol mol^{-1} and increased stepwise. For *E. camaldulensis*, CO_2 concentrations were set to 0, 50, 100, 150, 200, 300, 400, 600, 800, 1000, and 1200 μmol mol^{-1}. The CO_2 concentrations in A/C_i measurement in *N. tabacum* were set to 0, 50, 100, 150, 200, 300, 400, 600, 800, 1000, 1200, 1600, 2000 μmol mol^{-1}. Each stepwise measurement was completed within 2–3 min. Using A/C_i curves, we calculated the maximum rates of RuBP regeneration (J_{max}) and RuBP carboxylation (V_{cmax}) according to the method of Long and Bernacchi (2003). To identify the limiting step of CO_2 assimilation, we determined the chloroplast CO_2 concentration at which the transition from RuBP carboxylation to RuBP regeneration occurred (C_{trans}) as follows (Yamori et al., 2010, 2011):

$$C_{trans} = \frac{K_c(1 + O/K_o)J_{max}/4V_{cmax} - 2\Gamma^*}{1 - J_{max}/4V_{cmax}}$$

where K_c (μmol mol^{-1}) and K_o (mmol mol^{-1}) were the Michaelis constants for CO_2 and O_2, respectively (Farquhar et al., 1980), and were assumed to be 406.8 μmol mol^{-1} and 277 mmol mol^{-1}, respectively, at 25°C (Long and Bernacchi, 2003); O was the partial pressure of O_2 and was assumed to be 210 (Farquhar et al., 1980); J_{max} was the maximum rate of RuBP regeneration; and V_{cmax} was the maximum rate of RuBP carboxylation. The rate-limiting step for CO_2 assimilation was then determined by comparing the values of C_c and C_{trans}.

Modeling ATP Supplied via Flexible Mechanisms

The total amount of ATP demand from Rubisco carboxylation and oxygenation was obtained with the following formula (Walker et al., 2014):

$$v_{ATP} = \frac{(A_n + R_d)\,(3C_i + 3.5\frac{\Gamma^*}{\alpha})}{(C_i - \Gamma^*)}$$

Assuming that the stoichiometry of ATP/NADPH produced by LEF (electron transport from PSII to $NADP^+$) is 1.29 (Sacksteder et al., 2000; Seelert et al., 2000; Walker et al., 2014), the amount of ATP produced by LEF was calculated as:

$$v_{ATP(LEF)} = 1/2 \times J_g \times 1.29$$

Rates of ATP supply from other flexible mechanisms were determined by subtracting the amount of ATP produced by LEF from v_{ATP} according to:

$$v_{ATP(Flex)} = v_{ATP} - v_{ATP(LEF)}$$

Quantitative Limitation Analysis of A_n

Photosynthetic limitations in *E. camaldulensis* and *N. tabacum* were assessed according to the method of Grassi and Magnani (2005) and Carriqui et al. (2015). The values for stomatal (l_s), mesophyll conductance (l_{mc}), and biochemical (l_b) limitations represented measures of the relative importance of stomatal diffusion, mesophyll diffusion, and photosynthetic biochemistry in setting the observed value of A_n. Relative photosynthetic limitations were calculated as follows (Grassi and Magnani, 2005; Carriqui et al., 2015):

$$l_s = \frac{g_{tot}/g_s \times \partial A_n/\partial C_c}{g_{tot} + \partial A_n/\partial C_c}$$

$$l_{mc} = \frac{g_{tot}/g_m \times \partial A_n/\partial C_c}{g_{tot} + \partial A_n/\partial C_c}$$

$$l_b = \frac{g_{tot}}{g_{tot} + \partial A_n/\partial C_c}$$

where g_{tot} was total conductance to CO_2 between the leaf surface and carboxylation sites (calculated as $1/g_{tot} = 1/g_s + 1/g_m$).

Statistical Analysis

All results were displayed as mean values of four independent measurements. We used one-way ANOVA and SPSS 16.0 software (SPSS Inc., Chicago, IL, USA) to examine differences between the two species. Those differences were considered significant at $P < 0.05$.

RESULTS

A/C_i Curves and the Rate-Limiting Step of CO_2 Assimilation

The A/C_i curves indicated that the maximum rate of photosynthesis was higher in *N. tabacum* than in *E. camaldulensis* (**Figure 2A**). Values for the maximum rate of RuBP regeneration (J_{max}) and RuBP carboxylation (V_{cmax}) were significantly higher in *N. tabacum* (**Figure 2B**). Both species showed similar ratios of J_{max}/V_{cmax} (**Figure 1B**) as well as the same value for A_{400} at 400 μmol mol^{-1} CO_2. Because the CO_2 compensation point in the absence of daytime respiration (Γ^*) has an important impact on g_m, C_c, C_{trans}, and limitations on the stomata (l_s), mesophyll conductance (l_{mc}), and biochemical functions (l_b), we conducted a sensitivity analysis and examined the rate-limiting step for CO_2 assimilation to Γ^* (range from 30 to 40 μmol mol^{-1}). For *E. camaldulensis*, l_{mc} was the most important constraining factor for photosynthesis, followed by l_s and l_b (**Figure 2C**). By contrast, biochemical limitations were the most significant in *N. tabacum*, followed by l_{mc} and l_s (**Figure 2C**). Furthermore, irrespective of Γ^*, the value of C_c at 400 μmol mol^{-1} CO_2 was significantly lower than C_{trans} in *E. camaldulensis* (**Table 1**), suggesting that the rate-limiting step of A_{400} tended to be RuBP carboxylation. By comparison, in *N. tabacum* the value of C_c at 400 μmol mol^{-1} CO_2 was significantly higher than C_{trans} (**Table 1**), indicating A_{400} tended to be limited by RuBP regeneration.

Light Response Changes in CO_2 Assimilation and Photosynthetic Electron Flow

The light response curves demonstrated that the response of A_n to incident light was similar between *E. camaldulensis* and *N. tabacum* (**Figure 3A**). However, the maximum value of g_s was much higher in *E. camaldulensis* (**Figure 3B**), while C_i was slightly higher in that species (**Figure 3C**). When Γ^* was assumed to be 40 μmol mol^{-1}, then C_c under saturating light was much lower in *E. camaldulensis* (**Figure 3D**). At 2000 μmol photons m^{-2} s^{-1} in light response curves, the value of C_c was 124 μmol mol^{-1} in *E. camaldulensis* and 226 μmol mol^{-1} in *N. tabacum* (**Figure 3D**). This large difference of C_c between *E. camaldulensis* and *N. tabacum* was principally caused by the contrast in g_m.

Under all light intensities, *E. camaldulensis* had significantly higher effective quantum yield of PSII (Φ_{PSII}) compared to *N. tabacum*, especially under high light (**Figure 4A**). Concomitantly, NPQ values were lower in *E. camaldulensis* than *N. tabacum* (**Figure 4B**). According to the data of Φ_{PSII}, *E. camaldulensis* had significantly higher values of total electron

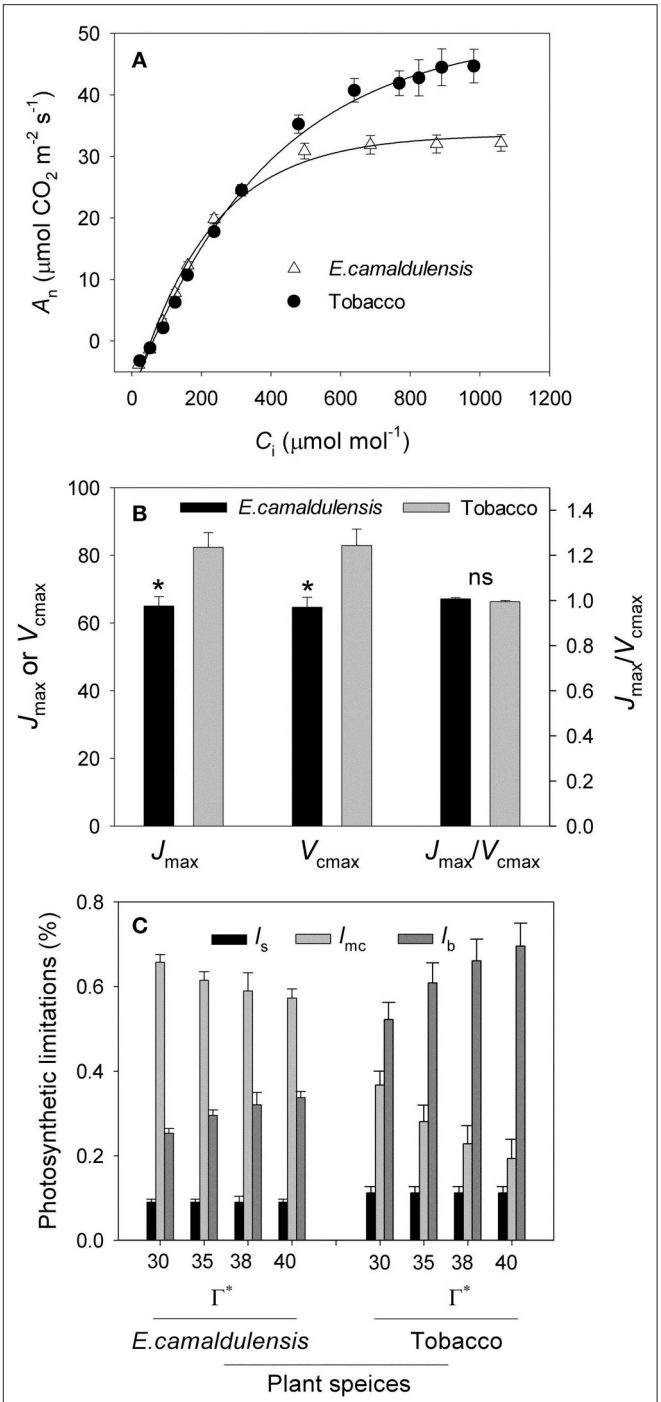

FIGURE 2 | Analysis of A/C_i curves and quantitative limitation analysis of A_n in *Eucalyptus camaldulensis* and *N. tabacum*. (A) Intercellular CO_2 concentration (C_i) response of CO_2 assimilation rate (A_n) in *Eucalyptus camaldulensis* and *N. tabacum* measured at 25°C and 1500 μmol photons m^{-2} s^{-1}. **(B)** Values for J_{max}, V_{cmax} and J_{max}/V_{cmax} ratio. J_{max} represents the maximum rate of RuBP regeneration; V_{cmax} indicates the maximum rate of RuBP carboxylation. **(C)** Sensitivity analyses of relative stomatal (l_s), mesophyll conductance (l_{mc}) and biochemical (l_b) limitations for photosynthesis to CO_2 compensation point under the absence of respiration condition (Γ^*) at 25°C and 400 μmol mol^{-1} CO_2. Values are means ± SE ($n = 4$).

TABLE 1 | Sensitivity analyses of rate-limiting step for CO_2 assimilation to Γ^*.

Species	Γ^*	g_m	C_c	C_{trans}	Significance between C_c and C_{trans}	A_r	A_c
E.camaldulensis	30	0.107	86.2	160.2	0.0001	−	+
	35	0.115	102.2	146.9	0.0001	−	+
	38	0.121	111.1	138.8	0.0001	−	+
	40	0.124	116.0	133.5	0.045	−	+
N. tabacum	30	0.194	185.1	156.6	0.01	+	−
	35	0.263	215.9	143.3	0.0001	+	−
	38	0.338	234.4	135.3	0.0001	+	−
	40	0.424	246.8	130.0	0.0001	+	−

Sensitivity analyses of photosynthetic parameters calculated from A/C_i curves to CO_2 compensation point in the absence of respiration condition (Γ^*) in Eucalyptus camaldulensis and N. tabacum. g_m, mesophyll conductance; C_c, chloroplast CO_2 concentration; C_{trans}, chloroplast CO_2 concentration at which the transition from RuBP carboxylation to RuBP regeneration occurs; A_r, RuBP regeneration; A_c, RuBP carboxylation. C_c for A_{400} less than C_{trans} indicates that CO_2 assimilation is limited by A_c, whereas C_c for A_{400} higher than C_{trans} indicates that CO_2 assimilation is limited by A_r. "−" represents no and "+" represents yes. Values are means ± SE (n = 4).

flow through PSII (J_T) than *N. tabacum* (**Figure 5A**). Meanwhile, the ratios of the rate of Rubisco carboxylation (V_c) to that of Rubisco oxygenation (V_o) under saturating light intensities were much higher in *E. camaldulensis* (**Figure 5B**). On assumptions of Γ^* being 40 μmol mol^{-1} and leaf absorbance being 0.85 in *E. camaldulensis* and *N. tabacum*, at 2000 μmol photons m^{-2} s^{-1}, comparative values for J_T and the V_o/V_c ratio in *E. camaldulensis* vs. *N. tabacum* were 280 vs. 178 and 0.63 vs. 0.38, respectively (**Figures 5A,B**). Furthermore, under light intensities above 300 μmol photons m^{-2} s^{-1}, electron flux for photorespiratory carbon oxidation [J_e(PCO)] were significantly higher in *E. camaldulensis* (**Figure 5C**). Values for J_e(PCO) at 2000 μmol photons m^{-2} s^{-1} were 100 and 48 μmol electrons m^{-2} s^{-1} in *E. camaldulensis* and *N. tabacum*, respectively. Plotting the V_o/V_c ratio and C_c indicated that the difference in the V_o/V_c ratio between *E. camaldulensis* and *N. tabacum* was mainly determined by the difference in C_c (**Figure 6**), which in turn caused by the change in g_m.

Alternative Electron Flow and ATP Synthesis from Flexible Mechanisms

Under high light, *E. camaldulensis* had significantly increased alternative electron flow, as indicated by the higher values of J_a and the J_a/J_g ratio (**Figure 7**). To examine the relationship between the alternative electron flow and photorespiration, we evaluated possible associations between J_a and J_e(PCO) under light intensities higher than 300 μmol photons m^{-2} s^{-1}. Interestingly, J_a was positively and linearly correlated with J_e(PCO) (**Figure 7A,** $P < 0.0001$). Similarly, the J_a/J_g ratio was positively and linearly correlated with V_o/V_c ratio (**Figure 7B,** $P < 0.0001$). According to photosynthesis model, an increase in the V_o/V_c ratio requires a higher ATP/NADPH energy demand from other flexible mechanisms such as cyclic electron flow and alternative electron flow. Increased alternative electron flow

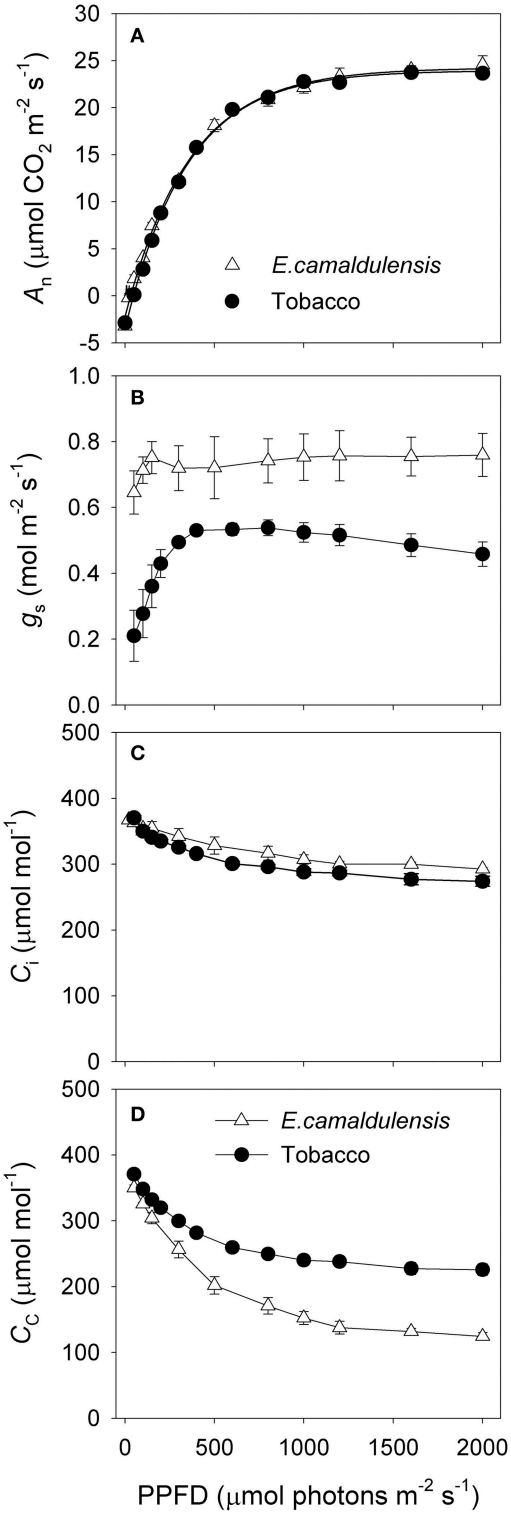

FIGURE 3 | Light response changes in (A) photosynthetic rate (A_n), **(B)** stomatal conductance (g_s), **(C)** intercellular CO_2 concentration (C_i), and **(D)** chloroplast CO_2 concentration (C_c) for leaves of *Eucalyptus camaldulensis* and *N. tabacum*. Measurements were conducted at 25°C and 400 μmol mol^{-1} CO_2. The value of C_c was based on the calculation of g_m on assumptions of Γ^* being 40 μmol mol^{-1} and L_{abs} being 0.85. Values are means ± SE ($n = 4$).

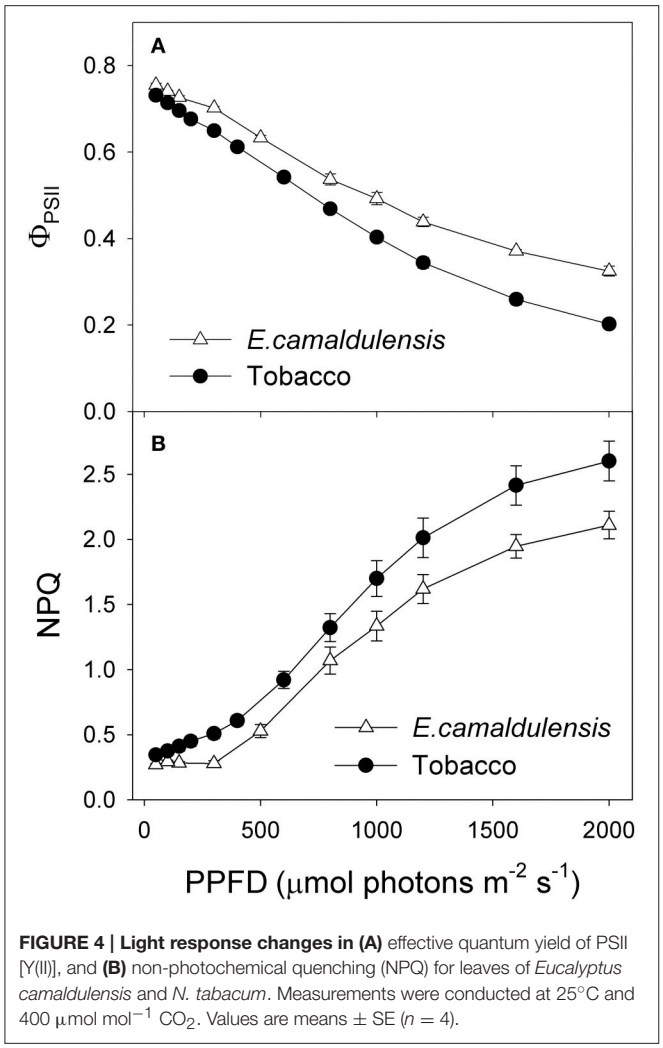

FIGURE 4 | Light response changes in (A) effective quantum yield of PSII [Y(II)], and **(B)** non-photochemical quenching (NPQ) for leaves of *Eucalyptus camaldulensis* and *N. tabacum*. Measurements were conducted at 25°C and 400 μmol mol^{-1} CO_2. Values are means ± SE ($n = 4$).

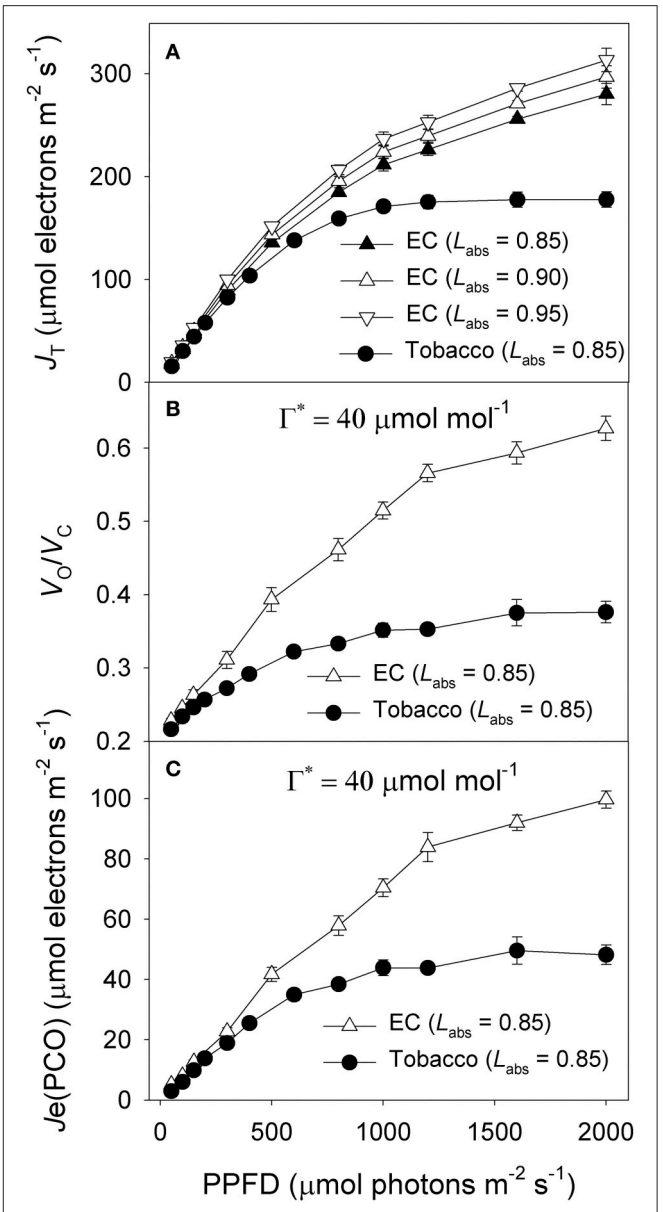

FIGURE 5 | Light response changes in (A) photosynthetic electron flow through PSII (J_T), and **(B)** the ratio of the rate of Rubisco carboxylation (V_C) to that of Rubisco oxygenation (V_O), and **(C)** electron flux for photorespiratory carbon oxidation [*Je*(PCO)] for leaves of *Eucalyptus camaldulensis* and *N. tabacum*. Measurements were conducted at 25°C and 400 μmol mol^{-1} CO_2. Values are means ± SE ($n = 4$).

promotes the formation of a proton gradient across the thylakoid membrane (ΔpH), which can be used for activating NPQ and ATP synthesis. We found that under high light the rate of ATP supplied from alternative electron sinks [$v_{ATP(Flex)}$] were much higher in *E. camaldulensis* than in *N. tabacum* (**Figure 8A**), and the rate of alternative electron flow was positively correlated to $v_{ATP(Flex)}$ (**Figure 8B**, $P < 0.0001$). Furthermore, NPQ values under high light were significantly lower in *E. camaldulensis* than in *N. tabacum* (**Figure 4B**), suggesting that the main role for alternative electron flow in *E. camaldulensis* is not to activate NPQ but to provide extra ATP. The greater capacity of the photorespiratory pathway in *E. camaldulensis* plants is sustained by the enhanced alternative electron flow.

DISCUSSION

In herbaceous C_3 crop species such as *N. tabacum*, spinach, rice and wheat, high stomatal and mesophyll conductance are essential for their strong photosynthetic capacities (Yamori et al., 2010, 2011). However, for sclerophyllous *Eucalyptus camaldulensis*, we found that its high rate of CO_2 assimilation (**Figure 3A**) was accompanied with a low g_m (≈0.12 molm^{-2} s^{-1}) (**Table 1**). Thus, high levels of mesophyll conductance do not appear to be a common mechanism for high rates of photosynthesis in C_3 plants. Surprisingly, in the sclerophyllous *E. camaldulensis*, the high rates of photosynthesis occurred at the low levels of C_c (**Figure 3D**), which directly increased the V_o/V_c ratio (**Figure 5B**). What is more, *E. camaldulensis* showed increased capacities of photorespiratory pathway (**Figure 5C**) and electron flow to alternative sinks (**Figure 7**). Enhancement of photorespiratory pathway increased

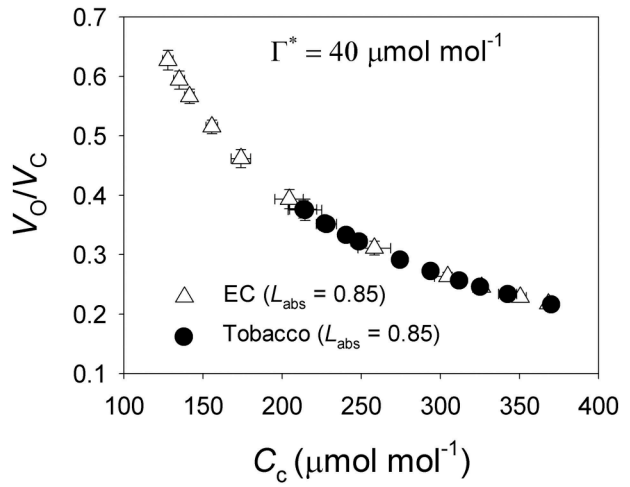

FIGURE 6 | The ratio of Rubisco oxygenation to carboxylation (V_O/V_C) as a function of C_C for leaves of *Eucalyptus camaldulensis* and *N. tabacum*. The data of V_O/V_C and C_C were referred from **Figures 2D**, **4B**, respectively. Values are means ± SE ($n = 4$).

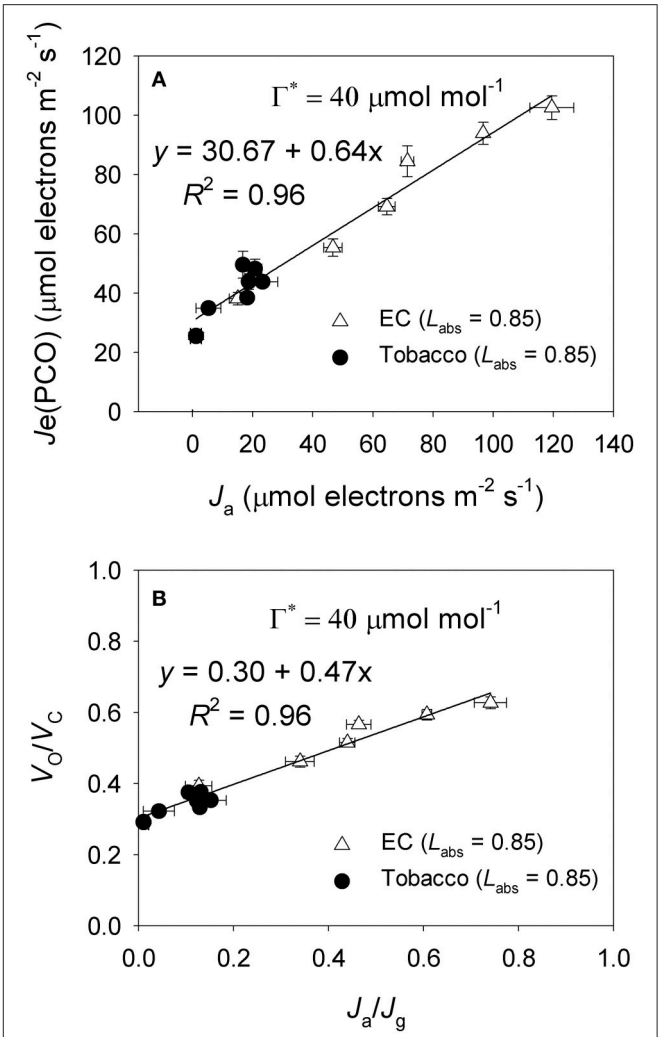

FIGURE 7 | (A) The value of *Je*(PCO) as a function of J_a (electron flux for alternative electron sinks) for leaves of *Eucalyptus camaldulensis* and tobacco; **(B)** The value of V_O/V_C as a function of J_a/J_g for leaves of *Eucalyptus camaldulensis* and tobacco. Data were obtained from light response curves (light intensities higher than 300 μmol photons m^{-2} s^{-1}) measured at 25°C and 400 μmol mol^{-1} CO_2. Values are means ± SE ($n = 4$). The coefficient of correlation (r) and significance of correlation (P) are 0.98 and <0.0001 for **Figure 6A**, respectively. The coefficient of correlation (r) and significance of correlation (P) are 0.98 and <0.0001 for **Figure 6B**, respectively.

the release of CO_2 in mitochondria. This photorespired CO_2 can be trapped and reassimilated by chloroplast, thereby boosting photosynthesis (Busch et al., 2013). Concomitantly, the increased photorespiratory pathway in *E. camaldulensis* needs more extra ATP supply from alternative electron sinks rather than electron transfer from water to $NADP^+$. Interestingly, the increased alternative electron flow provided essential extra ATP to balance the energy budget and sustain the high rate of photorespiratory pathway, then increasing the rate of photosynthetic CO_2 assimilation. These results highlight that the sclerophyllous *E. camaldulensis* enhanced the capacities of photorespiratory pathway and alternative electron flow to sustain a high rate of photosynthesis.

Quantitative Limitation Analysis of A_n

In *N. tabacum* leaves, l_b was the most important constraining factor for photosynthesis, followed by l_{mc} and l_s, being consistent with high levels of stomatal and mesophyll conductance. By comparison, in *E. camaldulensis*, l_{mc} had the greatest influence while l_s was the least limiting factor. This was consistent with the higher g_s and lower g_m measured for that species. These results confirmed that, the major limiting factor for photosynthesis differs intrinsically between high-photosynthesis herbaceous and sclerophyllous plants. Diffusional limitations of CO_2 are the main reason for lower photosynthetic rates in ferns than in angiosperms (Gago et al., 2013; Carriqui et al., 2015). Mesophyll conductance is the most constraining factor for photosynthesis in ferns (Carriqui et al., 2015). These findings suggested that, not only in low-photosynthesis species (e.g., ferns) but also in some high-photosynthesis sclerophyllous species such as *E. camaldulensis*, mesophyll conductance is the primary limiting factor for photosynthesis. The difference of g_m between *E. camaldulensis* and *N. tabacum* is probably determined by their leaf anatomy (Terashima et al., 2006). The thicker cell walls lead to a lower g_m in *E. camaldulensis* when compared with *N. tabacum*.

The Rate-Limiting Step of CO_2 Assimilation

The rate of CO_2 assimilation can be limited by RuBP carboxylation and/or RuBP regeneration in C_3 plants (Farquhar et al., 1980; Yamori et al., 2010, 2011). The specific rate-limiting step of CO_2 assimilation is determined by the relative values of C_c and C_{trans}. When the value of C_c is higher than C_{trans}, the CO_2 assimilation rate is mainly limited by RuBP regeneration. Otherwise, the CO_2 assimilation rate is limited by RuBP carboxylation when C_c is lower than C_{trans}. In *N. tabacum* leaves, the value of C_c under saturating light was higher

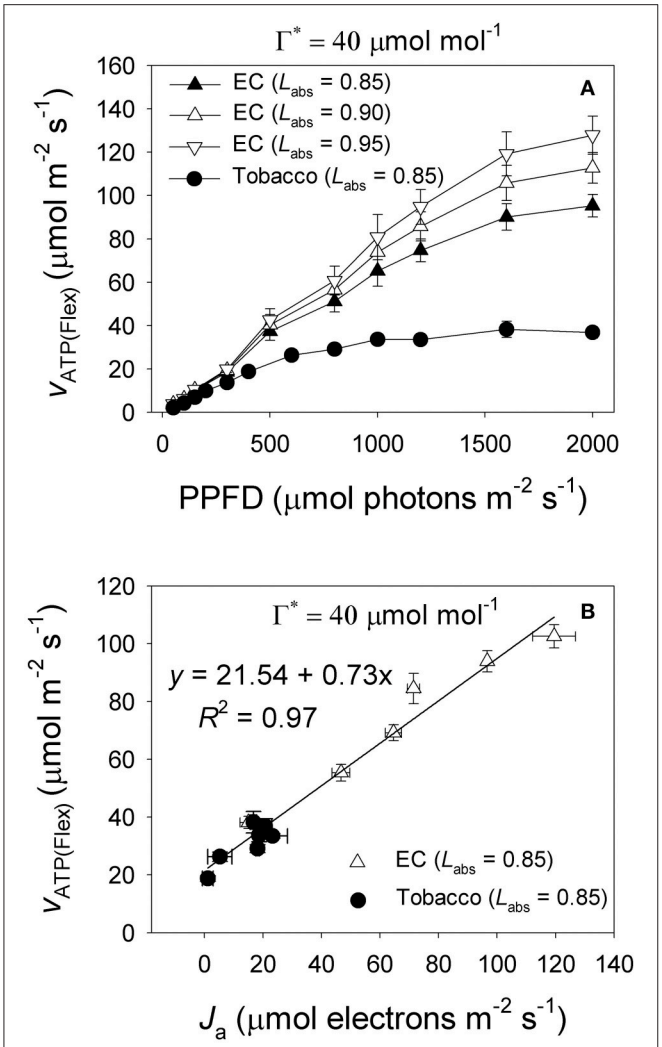

FIGURE 8 | (A) Light response change in the rate of ATP supplied from other flexible mechanisms rather than electron flow from water to $NADP^+$ [$v_{ATP(Flex)}$] for leaves of *Eucalyptus camaldulensis* and tobacco; **(B)** Relationship between the electron flux for alternative electron sinks (J_a) and $v_{ATP(Flex)}$ for leaves of *Eucalyptus camaldulensis* and tobacco, and data were obtained from light response curves (light intensities higher than 300 μmol photons m^{-2} s^{-1}) measured at 25°C and 400 μmol mol^{-1} CO_2. Values are means ± SE ($n = 4$). The coefficient of correlation (r) and significance of correlation (P) are 0.98 and <0.0001 for **Figure 7B**, respectively.

than C_{trans}, and thus the rate-limiting step of CO_2 assimilation tended to be RuBP regeneration (**Table 1**). On the contrary, the value of C_c under saturating light was lower than C_{trans} in *E. camaldulensis*, and thus the rate of CO_2 assimilation was limited by RuBP carboxylation (**Table 1**). According to the calculation of $C_c = C_i - A_n/g_m$, the value of C_c can be affected by three parameters C_i, A_n, and g_m. Here, because A_n and C_i values under saturating light were similar in *E. camaldulensis* and *N. tabacum* (**Figures 3A,C**), Because the value of C_c can be largely determined by g_m, the difference in the main rate-limiting step of CO_2 assimilation between *N. tabacum* and *E. camaldulensis* was mainly caused by the contrasts in their mesophyll conductance.

In the herbaceous *N. tabacum*, which has thin, flexible leaves, g_m can reach 0.5 mol m^{-2} s^{-1} when plants are exposed to high nitrogen concentrations (Yamori et al., 2011). By comparison, sclerophyllous plants have relatively lower g_m values that range between 0.09 and 0.25 mol m^{-2} s^{-1} (Lloyd et al., 1992; Hassiotou et al., 2009). Conductance in the mesophyll can be influenced by leaf anatomical traits such as the cell surface area and the chloroplast surface area that is exposed to intercellular air spaces (Evans et al., 1994; Oguchi et al., 2005; Terashima et al., 2011), chloroplast rearrangements (Tholen et al., 2008), cell wall thickness (Terashima et al., 2006, 2011; Flexas et al., 2012), and LMA (Flexas et al., 2008; Hassiotou et al., 2009). The value of LMA for in *E. camaldulensis* is approximately 169.5 g m^{-2} (Suganuma et al., 2006), which is much higher than *N. tabacum* (approximately 25 g m^{-2}) (Yamori et al., 2010). The large differences of leaf anatomical traits between *E. camaldulensis* and *N. tabacum* might result in the diversity of g_m.

Photorespiration

We found that the capacity of the photorespiratory pathway was greater for *E. camaldulensis* than for *N. tabacum* (**Figures 5B,C**). Rubisco is a dual functional enzyme that catalyzes the carboxylation of RuBP, but also oxygenates RuBP in photorespiration. A lower C_c in *E. camaldulensis* would increase the rate of RuBP oxygenation by Rubisco. Photorespiration begins with RuBP oxygenation that generates glycolate-2-phosphate and glycerate-3-phosphateare. To maintain a steady-state high rate of photosynthesis in *E. camaldulensis*, the RuBP pool must remain stable. In chloroplast, the steady-state of RuBP pool depends on two different RuBP regeneration pathways: the Calvin-Benson cycle and the photorespiratory pathway. Impairment of photorespiratory pathway induced a gradient decrease in photosynthetic rate at atmospheric CO_2 concentration (Takahashi et al., 2007). Importantly, during steady-state phases, the rates of RuBP oxygenation and RuBP regeneration through the photorespiratory pathway must be balanced. Under high light, *E. camaldulensis* accelerate the photorespiratory pathway to favor the regeneration of RuBP via glycerate-3-phosphate, thereby preventing the RuBP pool from shrinking.

A reduction in C_c also accelerates the production of photorespiratory intermediates, e.g., glycine and glycerate, which inhibit the Calvin-Benson cycle (Chastain and Ogren, 1989; Eisenhut et al., 2007; Timm et al., 2012, 2015). In *Arabidopsis thaliana* plants with elevated glycine decarboxylase activity, the rapid acceleration of the photorespiratory pathway lowers the accumulation of photorespiratory metabolites including those which impair Rubisco activation and possibly the activity of other enzymes of the Calvin-Benson cycle, increasing the performance of the Calvin-Benson cycle (Timm et al., 2012, 2015). Furthermore, *N. tabacum* plants grown under high light and high nitrogen concentration up-regulate photorespiratory pathway to maintain high rates of photosynthesis (Huang et al., 2014, 2016). To overcome those detrimental effects, the photorespiratory pathway should be enhanced in *E. camaldulensis*. In addition, although CO_2

is released in the mitochondria in the photorespiratory pathway, C_3 plants can trap photorespired CO_2 within individual mesophyll cell. This causes chloroplast CO_2 concentrations to rise and, ultimately, improves the rate of photosynthesis in C_3 plants (Busch et al., 2013). Taking together, the enhanced photorespiratory capacity strongly contributes to the high rate of CO_2 assimilation in *E. camaldulensis*.

Alternative Electron Flow

We were surprised to learn that, under saturating illumination, alternative electron flow was enhanced in *E. camaldulensis* when compared with *N. tabacum*. The water-water cycle, nitrate reduction and malate shunt are potential candidates responsible for this increase in alternative electron flow (Yi et al., 2014). When plants are illuminated at atmospheric CO_2 and O_2, most of this alternative flow accounts for the electron flux to oxygen and oxidized ascorbic acid (Miyake and Yokota, 2000; Makino et al., 2002). Thus, we concluded that the WWC activity was greater in *E. camaldulensis*. During the early phase of photosynthetic induction in rice, the WWC first generates a ΔpH across the thylakoid membranes to form NPQ and supply ATP for carbon assimilation (Neubauer and Yamamoto, 1992; Miyake and Yokota, 2000; Makino et al., 2002). However, when photosynthesis reaches a steady-state rate, the WWC no longer maintains a high NPQ but instead provides additional ATP for primary metabolism in rice leaves (Makino et al., 2002). Our light response curves indicated that NPQ values under high light were significantly lower in *E. camaldulensis* (**Figure 4B**). Because the NPQ activation relies on the acidification of thylakoid lumen, and which also depresses electron transport through Cyt b_6/f complex via "photosynthetic control," this result suggested the higher levels of lumen acidification in leaves of *N. tabacum* when illuminated at high light. Therefore, the steady-state rate of WWC under intense illumination in *E. camaldulensis* mainly contributed to additional ATP synthesis rather than lumen acidification, which is consistent with previous studies on the role of the WWC (Makino et al., 2002; Huang et al., 2016).

In electron flow from PSII to $NADP^+$, the stoichiometry of the ATP/NADPH ratio is thought to be 1.29 (Sacksteder et al., 2000; Seelert et al., 2000). By comparison, each Rubisco oxygenation consumes 3.5 ATP and 2 NADH equivalents in total. Therefore, the occurrence of photorespiratory pathway needs a higher ATP/NADPH ratio than 1.29 to maintain primary metabolism (Edwards and Walker, 1983; Walker et al., 2014). Under high light and ambient CO_2, the ATP/NADPH ratio required by CO_2 assimilation, photorespiration, and nitrite assimilation is approximately 1.6 (Walker et al., 2014). Furthermore, the ATP/NADPH energy demand for primary metabolism will rise as photorespiration increases. As a result, the rate of ATP supplied from other flexible pathways must be higher in *E. camaldulensis* due to its higher rate of photorespiratory pathway. Cyclic electron flow and the WWC are the main flexible pathways that contribute to extra ATP synthesis under high light and atmospheric CO_2 concentrations (Makino et al., 2002; Walker et al., 2014; Huang et al., 2015, 2016). Here, we found that the greater rate of photorespiration was accompanied by higher alternative electron flow (**Figure 7**), and the rate of ATP supplied from other flexible mechanisms was positively correlated to the rate of electron flow to alternative sinks (**Figure 8B**). Therefore, it appears that *E. camaldulensis* enhances the alternative electron flow to balance the ATP/NADPH energy demand for high rates of photorespiration.

CONCLUSIONS

In order to illustrate the potential different mechanisms underlying the high rates of photosynthesis in sclerophyllous and herbaceous C_3 plants. Gas exchange and chlorophyll fluorescence were measured in *E. camaldulensis* (sclerophyllous) and *N. tabacum* (herbaceous). Although *E. camaldulensis* and *N. tabacum* had similar A_n under saturating light, the value of g_m differed largely between *N. tabacum* and *E. camaldulensis*. In *N. tabacum*, a higher g_m increased the value of C_c, resulting in the rate-limiting step of CO_2 assimilation tended to be RuBP regeneration. On the contrary, RuBP carboxylation was the main rate-limiting step of CO_2 assimilation in *E. camaldulensis* because CO_2 diffusion to the chloroplasts was restricted by a lower g_m. Therefore, the rate-limiting step of CO_2 assimilation appears to be more related to g_m rather than g_s in high-photosynthesis species. The lower C_c aggravated RuBP oxygenation in *E. camaldulensis*. Meanwhile, increased flux through the photorespiratory pathway minimizes the accumulation of photorespiratory metabolites, benefiting photosynthetic CO_2 fixation in the Calvin-Benson cycle in *E. camaldulensis*. In order to balance the ATP/NADPH energy demand for high rates of photorespiration, *E. camaldulensis* up-regulated alternative electron flow to provide extra ATP. Thus, coordination of photorespiratory pathway and alternative electron flow is crucial for the high rates of CO_2 assimilation in *E. camaldulensis*. These results highlight the different mechanisms responsible for high rates of photosynthesis in the sclerophyllous plant *E. camaldulensis* and the herbaceous plant *N. tabacum*.

AUTHOR CONTRIBUTIONS

WH and YT conceived and designed research. WH conducted experiments. WH, GY, and WY analyzed data. WH wrote the manuscript.

ACKNOWLEDGMENTS

This work was supported by the National Natural Science Foundation of China (Grant 31300332), and Youth Innovation Promotion Association of the Chinese Academy of Sciences.

REFERENCES

Asada, K. (1999). The water-water cycle in chloroplasts: scavenging of active oxygens and dissipation of excess photons. *Annu. Rev. Plant Biol.* 50, 601–639. doi: 10.1146/annurev.arplant.50.1.601

Asada, K. (2000). The water–water cycle as alternative photon and electronsinks. *Phil. Trans. R. Soc. Lond. B.* 355, 1419–1431. doi: 10.1098/rstb.2000.0703

Baker, N. R., and Rosenqvist, E. (2004). Applications of chlorophyll fluorescence can improve crop production strategies: an examination of future possibilities. *J. Exp. Bot.* 55, 1607–1621. doi: 10.1093/jxb/erh196

Brooks, A., and Farquhar, G. D. (1985). Effect of temperature on the CO_2/O_2 specificity of ribulose-1,5-bisphosphate carboxylase/oxygenase and the rate of respiration in the light. *Planta* 165, 397–406. doi: 10.1007/BF00392238

Busch, F. A., Sage, T. L., Cousins, A. B., and Sage, R. F. (2013). C_3 plants enhance rates of photosynthesis by reassimilating photorespired and respired CO_2. *Plant Cell Environ.* 36, 200–212. doi: 10.1111/j.1365-3040.2012.02567.x

Carriqui, M., Cabrera, H. M., Conesa, M. Á., Coopman, R. E., Douthe, C., Gago, J., et al. (2015). Diffusional limitations explain the lower photosynthetic capacity of ferns as compared with angiosperms in a common garden study. *Plant Cell Environ.* 38, 448–460. doi: 10.1111/pce.12402

Chastain, C. J., and Ogren, W. L. (1989). Glyoxylate inhibition of ribulosebisphosphate carboxylase/oxygenase activation state *in vivo*. *Plant Cell Physiol.* 30, 937–944.

Edwards, G. E., and Walker, D. A. (1983). *C3, C4: Mechanisms, and Cellular and Environmental Regulation, of Photosynthesis*. Oxford; London: Blackwell Scientific.

Eisenhut, M., Bauwe, H., and Hagemann, M. (2007). Glycine accumulation is toxic for the cyanobacterium *Synechocystis* sp. strain PCC 6803, but can be compensated by supplementation with magnesium ions. *FEMS. Microbiol. Lett.* 277, 232–237. doi: 10.1111/j.1574-6968.2007.00960.x

Evans, J. R. (1987). The relationship between electron transport components and photosynthetic capacity in pea leaves grown at different irradiances. *Aust. J. Plant Physiol.* 14, 157–170. doi: 10.1071/pp9870157

Evans, J. R., von Caemmerer, S., Setchell, B. A., and Hudson, G. S. (1994). The relationship between CO_2 transfer conductance and leaf anatomy in transgenic tobacco with a reduced content of Rubisco. *Funct. Plant Biol.* 21, 475–495.

Farquhar, G. D., von Caemmerer, S., and Berry, J. A. (1980). A biochemical model of photosynthetic CO_2 assimilation in leaves of C_3 species. *Planta* 149, 78–90. doi: 10.1007/BF00386231

Flexas, J., Barbour, M. M., Brendel, O., Cabrera, H. M., Carriqui, M., Díaz-Espejo, A., et al. (2012). Mesophyll diffusion conductance to CO_2: an unappreciated central player in photosynthesis. *Plant Sci.* 193–194, 70–84. doi: 10.1016/j.plantsci.2012.05.009

Flexas, J., Bota, J., Escalona, J. M., Sampol, B., and Medrano, H. (2002). Effects of drought on photosynthesis in grapevines under field conditions: an evaluation of stomatal and mesophyll limitations. *Funct. Plant Biol.* 29, 461–471. doi: 10.1071/pp01119

Flexas, J., and Medrano, H. (2002). Energy dissipation in C_3 plants under drought. *Funct. Plant Biol.* 29, 1209–1215. doi: 10.1071/fp02015

Flexas, J., Ribas-Carbó, M., Díaz-Espejo, A., Galmés, J., and Medrano, H. (2008). Mesophyll conductance to CO_2: current knowledge and future prospects. *Plant Cell Environ.* 31, 602–621. doi: 10.1111/j.1365-3040.2007.01757.x

Gago, J., Coopman, R. E., Cabrera, H. M., Hermida, C., Molins, A., Conesa, M. A., et al. (2013). Photosynthesis limitations in three fern species. *Physiol. Plant* 149, 599–611. doi: 10.1111/ppl.12073

Genty, B., Briantais, J. M., and Baker, N. R. (1989). The relationship between the quantum yield of photosynthetic electron transport and quenching of chlorophyll fluorescence. *Biochim. Biophys. Acta* 99, 87–92. doi: 10.1016/s0304-4165(89)80016-9

Grassi, G., and Magnani, F. (2005). Stomatal, mesophyll conductance and biochemical limitations to photosynthesis as affected by drought and leaf ontogeny in ash and oak trees. *Plant Cell Environ.* 28, 834–849. doi: 10.1111/j.1365-3040.2005.01333.x

Hanba, Y. T., Kogami, H., and Terashima, I. (2002). The effect of growth irradiance on leaf anatomy and photosynthesis in *Acer* species differing in light demand. *Plant Cell Environ.* 25, 1021–1030. doi: 10.1046/j.1365-3040.2002.00881.x

Harley, P. C., Loreto, F., Marco, G. D., and Sharkey, T. D. (1992). Theoretical considerations when estimating the mesophyll conductance to CO_2 flux by analysis of the response of photosynthesis to CO_2. *Plant Physiol.* 98, 1429–1436. doi: 10.1104/pp.98.4.1429

Hassiotou, F., Ludwig, M., Renton, M., Veneklaas, E. J., and Evans, J. R. (2009). Influence of leaf dry mass per area, CO_2, and irradiance on mesophyll conductance in sclerophylls. *J. Exp. Bot.* 60, 2303–2314. doi: 10.1093/jxb/erp021

Hikosaka, K. (1996). Effects of leaf age, nitrogen nutrition and photon flux density on the organization of the photosynthetic apparatus in leaves of a vine (*Ipomoea tricolor* Cav.). grown horizontally to avoid mutual shading of leaves. *Planta* 198, 144–150.

Hikosaka, K., and Terashima, I. (1996). Nitrogen partitioning among photosynthetic components and its consequence in sun and shade plants. *Funct. Ecol.* 10, 335–343.

Huang, W., Yang, Y.-J., Hu, H., and Zhang, S.-B. (2015). Different roles of cyclic electron flow around photosystem I under sub-saturating and saturating light intensities in tobacco leaves. *Front. Plant Sci.* 6:923. doi: 10.3389/fpls.2015.00923

Huang, W., Yang, Y.-J., Hu, H., and Zhang, S.-B. (2016). Different roles of cyclic electron flow around photosystem I under sub-saturating and saturating light intensities in tobacco leaves. *Front. Plant Sci.* 157, 97–104. doi: 10.3389/fpls.2015.00923

Huang, W., Zhang, S.-B., and Hu, H. (2014). Sun leaves up-regulate the photorespiratory pathway to maintain a high rate of CO_2 assimilation in tobacco. *Front. Plant Sci.* 5:688. doi: 10.3389/fpls.2014.00688

Krall, J. P., and Edwards, G. E. (1992). Relationship between photosystem II activity and CO_2 fixation in leaves. *Physiol. Plant* 86, 180–187.

Lloyd, J., Syvertsen, J. P., Kriedemann, P. E., and Farquhar, G. D. (1992). Low conductances for CO_2 diffusion from stomata to the sites of carboxylation in leaves of woody species. *Plant Cell Environ.* 15, 873–899.

Long, S. P., and Bernacchi, C. J. (2003). Gas exchange measurements, what can they tell us about the underlying limitations to photosynthesis? Procedures and sources of error. *J. Exp. Bot.* 54, 2393–2401. doi: 10.1093/jxb/erg262

Loreto, F., Harley, P. C., Marco, G. D., and Sharkey, T. D. (1992). Estimation of mesophyll conductance to CO_2 flux by three different methods. *Plant Physiol.* 98, 1437–1443.

Makino, A., Miyake, C., and Yokota, A. (2002). Physiological functions of the water–water cycle (Mehler reaction). and the cyclic electron flow around PSI in rice leaves. *Plant Cell Physiol.* 43, 1017–1026. doi: 10.1093/pcp/pcf124

Miyake, C., and Yokota, A. (2000). Determination of the rate of photoreduction of O_2 in the water-water cycle in watermelon leaves and enhancement of the rate by limitation of photosynthesis. *Plant Cell Physiol.* 41, 335–343. doi: 10.1093/pcp/41.3.335

Neubauer, C., and Yamamoto, H. (1992). Mehler-peroxidase reaction mediates zeaxanthin formation and zeaxanthin-related fluorescence quenching in intact chloroplasts. *Plant Physiol.* 99, 1354–1361. doi: 10.1104/pp.99.4.1354

Oguchi, R., Hikosaka, K., and Hirose, T. (2003). Does the photosynthetic light-acclimation need change in leaf anatomy? *Plant Cell Environ.* 26, 505–512. doi: 10.1046/j.1365-3040.2003.00981.x

Oguchi, R., Hikosaka, K., and Hirose, T. (2005). Leaf anatomy as a constraint for photosynthetic acclimation: differential responses in leaf anatomy to increasing growth irradiance among three deciduous trees. *Plant Cell Environ.* 28, 916–927. doi: 10.1111/j.1365-3040.2005.01344.x

Sacksteder, C. A., Kanazawa, A., Jacoby, M. E., and Kramer, D. M. (2000). The proton to electron stoichiometry of steady-state photosynthesis in living plants: a proton-pumping Q cycle is continuously engaged. *Proc. Natl. Acad. Sci. U.S.A.* 97, 14283–14288. doi: 10.1073/pnas.97.26.14283

Seelert, H., Poetsch, A., Dencher, N. A., Engel, A., Stahlberg, H., and Müller, D. J. (2000). Proton-powered turbine of a plant motor. *Nature* 405, 418–419. doi: 10.1111/j.1399-3054.1988.tb09205.x

Sharkey, T. D. (1988). Estimating the rate of photorespiration in leaves. *Physiol. Plant* 73, 147–152.

Somerville, C. R., and Ogren, W. L. (1980). Inhibition of photosynthesis in *Arabidopsis* mutants lacking leaf glutamate synthase activity. *Nature* 286, 257–259.

Somerville, C. R., and Ogren, W. L. (1981). Photorespiration-deficient mutants of *Arabidopsis thaliana* lacking mitochondrial serine transhydroxymethylase activity. *Plant Physiol.* 67, 666–671.

Somerville, C. R., and Ogren, W. L. (1983). An *Arabidopsis thaliana* mutant defective in chloroplast dicarboxylate transport. *Proc. Natl. Acad. Sci. U.S.A.* 80, 1290–1294.

Suganuma, H., Abe, Y., Taniguchi, M., Tanouchi, H., Utsugi, H., Kojima, T., et al. (2006). Stand biomass estimation method by canopy coverage for application to remote sensing in an arid area of Western Australia. *Forest Ecol. Manage* 222, 75–87. doi: 10.1016/j.foreco.2005.10.014

Takahashi, S., Bauwe, H., and Badger, M. R. (2007). Impairment of the photorespiratory pathway accelerates photoinhibition of photosystem II by suppression of repair but not acceleration of damage processes in *Arabidopsis*. *Plant Physiol.* 144, 487–494. doi: 10.1104/pp.107.097253

Terashima, I., and Evans, J. R. (1988). Effects of light and nitrogen nutrition on the organization of the photosynthetic apparatus in spinach. *Plant Cell Physiol.* 29, 143–155.

Terashima, I., Hanba, Y. T., Tazoe, Y., Vyas, P., and Yano, S. (2006). Irradiance and phenotype: comparative eco-development of sun and shade leaves in relation to photosynthetic CO_2 diffusion. *J. Exp. Bot.* 57, 343–354. doi: 10.1093/jxb/erj014

Terashima, I., Hanba, Y. T., Tholen, D., and Niinemets, Ü. (2011). Leaf functional anatomy in relation to photosynthesis. *Plant Physiol.* 155, 108–116. doi: 10.1104/pp.110.165472

Tholen, D., Boom, C., Noguchi, K., Ueda, S., Katase, T., and Terashima, I. (2008). The chloroplast avoidance response decreases internal conductance to CO_2 diffusion in *Arabidopsis thaliana* leaves. *Plant Cell Environ.* 31, 1688–1700. doi: 10.1111/j.1365-3040.2008.01875.x

Timm, S., Florian, A., Arrivault, S., Stitt, M., and Fernie, A. R. (2012). Glycine decarboxylase controls photosynthesis and plant growth. *FEBS Lett.* 586, 3692–3697. doi: 10.1016/j.febslet.2012.08.027

Timm, S., Wittmiß, M., Gamlien, S., Ewald, R., Florian, A., Frank, M., et al. (2015). Mitochondrial dihydrolipoyl dehydrogenase activity shapes photosynthesis and photorespiration of *Arabidopsis thaliana*. *Plant Cell* 27, 1968–1984. doi: 10.1105/tpc.15.00105

von Caemmerer, S. (2000). *Biochemical Models of Leaf Photosynthesis*. Collingwood, VIC: CSIRO Publishing.

von Caemmerer, S., and Farquhar, G. D. (1981). Some relationships between the biochemistry of photosynthesis and the gas exchange of leaves. *Planta* 153, 376–387.

Walker, B. J., Strand, D. D., Kramer, D. M., and Cousins, A. B. (2014). The response of cyclic electron flow around photosystem I to changes in photorespiration and nitrate assimilation. *Plant Physiol.* 165, 453–462. doi: 10.1104/pp.114.238238

Walker, B. J., VanLoocke, A., Bernacchi, C. J., and Ort, D. R. (2016). The costs of photorespiration to food production now and in the future. *Annu. Rev. Plant Biol.* 67,107–129. doi: 10.1146/annurev-arplant-043015-111709

Warren, C. R., and Dreyer, E. (2006). Temperature response of photosynthesis and internal conductance to CO_2: results from two independent approaches. *J. Exp. Bot.* 57, 3057–3067. doi: 10.1093/jxb/erl067

Yamori, W., Evans, J. R., and von Caemmerer, S. (2010). Effects of growth and measurement light intensities on temperature dependence of CO_2 assimilation rate in tobacco leaves. *Plant Cell Environ.* 33, 332–343. doi: 10.1111/j.1365-3040.2009.02067.x

Yamori, W., Nagai, T., and Makino, A. (2011). The rate-limiting step for CO_2 assimilation at different temperatures is influenced by the leaf nitrogen content in several C_3 crop species. *Plant Cell Environ.* 34, 764–777. doi: 10.1111/j.1365-3040.2011.02280.x

Yi, X.-P., Zhang, Y.-L., Yao, H.-S., Zhang, X.-J., Luo, H.-H., Gou, L., et al. (2014). Alternative electron sinks are crucial for conferring photoprotection in field-grown cotton under water deficit during flowering and boll setting stages. *Funct. Plant Biol.* 41, 737–747. doi: 10.1071/fp13269

Zivcak, M., Brestic, M., Balatova, Z., Drevenakova, P., Olsovska, K., Kalaji, H. M., et al. (2013). Photosynthetic electron transport and specific photoprotective responses in wheat leaves under drought stress. *Photosynth. Res.* 117, 529–546. doi: 10.1007/s11120-013-9885-3

Conflict of Interest Statement: The authors declare that the research was conducted in the absence of any commercial or financial relationships that could be construed as a potential conflict of interest.